

CLSM as Quantitative Method to Determine the Size of Drug Crystals in a Solid Dispersion

Hans de Waard · Martin J. T. Hessels · Maarten Boon · Klaas A. Sjollema · Wouter L. J. Hinrichs · Anko C. Eissens · Henderik W. Frijlink

Received: 21 September 2010 / Accepted: 16 May 2011 / Published online: 24 May 2011
© The Author(s) 2011. This article is published with open access at Springerlink.com

ABSTRACT

Purpose To test whether confocal laser scanning microscopy (CLSM) can be used as an analytical tool to determine the drug crystal size in a powder mixture or a crystalline solid dispersion.

Methods Crystals of the autofluorescent drug dipyrindamole were incorporated in a matrix of crystalline mannitol by physical mixing or freeze-drying. Laser diffraction analysis and dissolution testing were used to validate the particle size that was found by CLSM.

Results The particle size of the pure drug as determined by laser diffraction and CLSM were similar (D_{50} of approximately $22 \mu\text{m}$). CLSM showed that the dipyrindamole crystals in the crystalline dispersion obtained by freeze-drying of less concentrated solutions were of sub-micron size ($0.7 \mu\text{m}$), whereas the crystals obtained by freeze-drying of more concentrated solutions were larger ($1.3 \mu\text{m}$). This trend in drug crystal size was in agreement with the dissolution behavior of the tablets prepared from these products.

Conclusion CLSM is a useful technique to determine the particle size in a powder mixture. Furthermore, CLSM can be used to determine the drug crystal size over a broad size distribution. A limitation of the method is that the drug should be autofluorescent.

KEY WORDS confocal laser scanning microscopy · controlled crystallization during freeze-drying · dipyrindamole · dissolution · freeze-drying

INTRODUCTION

Many new drug candidates can be categorized as class II drugs according to the Biopharmaceutics Classification System (1). These drugs have a low aqueous solubility, but once they are dissolved, they are easily absorbed over the gastro-intestinal membrane (2,3). Since dissolution is the rate limiting step for absorption for these drugs, the bioavailability can be improved by increasing the dissolution rate (4). A strategy to increase the dissolution rate is the application of drug nanocrystals (5–8). According to the Ostwald-Freundlich equation (9) and the Noyes-Whitney equation (10), the dissolution rate of drug nanocrystals is increased due to an increased saturation concentration around the small particles and due to an increased surface to volume ratio.

Previously, we developed a novel bottom-up process to produce such drug nanocrystals: controlled crystallization during freeze-drying (CCDF) (11). Briefly, a drug and a matrix material, dissolved in a mixture of tertiary butyl alcohol (TBA) and water was rapidly frozen and then freeze-dried. Freeze-drying was performed at a relatively high temperature to allow both drug and matrix to crystallize (12). By using this process, nanocrystalline dispersions with improved dissolution behavior were obtained.

Usually, methods such as dynamic light scattering (DLS) and laser diffraction are used to measure the size of nanoparticles. Disadvantages of these methods are that when DLS is used, only the submicron particles can be

H. de Waard (✉) · M. J. T. Hessels · M. Boon · W. L. J. Hinrichs · A. C. Eissens · H. W. Frijlink
Department of Pharmaceutical Technology and Biopharmacy
University of Groningen
Antonius Deusinglaan 1, 9713 AV Groningen, The Netherlands
e-mail: h.de.waard@rug.nl

K. A. Sjollema
Microscopy and Imaging Center
University Medical Center Groningen
Antonius Deusinglaan 1, 9713 AV Groningen, The Netherlands

measured (13). And when laser diffraction is used, it is difficult to apply the correct optimal parameters (14). Nevertheless, these methods could provide accurate particle size distributions of nanosuspensions. However, to be able to measure nanoparticles with these methods, the particles should be dispersed in a liquid. When top-down methods, such as high pressure homogenization or wet ball milling, are used, the obtained product is a nanosuspension. However, when CCDF is used to prepare drug nanocrystals, the particles should be dispersed in a liquid first. In order to determine the size of the drug particles in the matrix, the matrix material should dissolve in the liquid, but the drug should not. Unfortunately, when the crystalline dispersions are dispersed in aqueous or non-aqueous solvents, the drug particles can easily agglomerate or dissolve rapidly (15). Agglomeration can be prevented by the addition of surfactants. However, surfactants can cause drugs to partially dissolve. This effect can lead to the formation of sub-optimal crystal sizes (15,16).

If the particle size of the drug in the matrix could be determined in solid state, these drawbacks would be overcome. A frequently used method to distinguish between different components in solid state is energy-dispersive X-ray spectroscopy (EDX). For this method, it is required that the different molecules in the mixture contain different types of atoms and, preferably, that the deviating atom has a high atomic mass. However, frequently, the atomic mass or the concentration of the deviating atoms in the drug is too low, or there are no deviating atoms at all. For example, in a previous study (11), we used fenofibrate and mannitol as model drug and matrix, respectively. The only atom type in fenofibrate that is absent in mannitol is chloride. Since there is only one chloride atom per molecule fenofibrate and the atomic mass of chloride is low, EDX could not be used to determine the drug crystal size.

Other methods that potentially could be used to distinguish the drug from the matrix are Raman spectroscopy or confocal laser scanning microscopy (CLSM). Both techniques are used to determine the size distribution of a drug in a mixture (17). At optimal conditions, the spatial resolution of both techniques is approximately 0.25 μm (18,19), which makes both techniques suitable to measure particles in the sub-micron range. When Raman spectroscopy is used, the characteristic peaks of both components should not overlap; otherwise, discrimination of drug from the matrix is impossible. On the other hand, to be able to distinguish between the drug from the matrix when CLSM is used, the drug of interest or the matrix material should be autofluorescent. Since there are many examples of autofluorescent drugs (e.g. dipyrindamole, nifedipine, tetracyclines, and acridines), CLSM could be a useful method to determine the drug particle size.

The aim of this study was to focus on CLSM and to test whether this technique can be used to determine the drug crystal size in the solid state. In order to test this, drug crystals of a poorly soluble and autofluorescent drug were prepared by CCDF. Dipyrindamole was selected as model drug, because it can be categorized as BCS class II drug (logP: 3.95 (20); aqueous solubility at neutral pH: 38 mg/L (21)), and it is autofluorescent due to its aromatic ring system (22).

MATERIALS AND METHODS

Materials

Dipyrindamole and TBA were obtained from Sigma-Aldrich Chemie B.V. Zwijndrecht, The Netherlands. Mannitol was obtained from Roquette (France). Fluorescent TetraSpeck™ microspheres were obtained from Invitrogen Life Science. Demineralized water was used in all experiments.

Methods

Preparation of the Crystalline Dispersions

The controlled crystallized dispersions were prepared according to the method described previously (11). Briefly, two separate solutions of dipyrindamole in TBA and mannitol in water were prepared (for compositions see Table I). Both solutions were heated to approximately 60°C and mixed in a glass vial. Immediately after mixing, the solutions were frozen by placing them on a pre-cooled (−50°C) shelf of a freeze-dryer (Christ model Epsilon 2–4 lyophilizer, Breukelen, the Netherlands). This temperature was maintained for 1.5 h, after which the temperature was increased at a rate of 1°C/min to −25°C to allow the drug and matrix to crystallize during a period of three hours. Then, the samples were dried for 10 h at 0.220 mBar. Finally, the temperature was gradually increased to room temperature. The obtained powders were stored in a desiccator over silica gel at room temperature for at least one day before further processing.

Table I Composition of the Different Solutions Used to Prepare the Controlled Crystallized Dispersions. In All Experiments, 1.2 mL Aqueous Solution was Mixed With 0.8 mL TBA Solution (i.e. ratio of 6/4)

Before lyophilization		After lyophilization
$C_{\text{dipyrindamole/TBA}}$ (mg/ml)	$C_{\text{mannitol/water}}$ (mg/ml)	Drug/matrix ratio
25.0	150	10/90
50.0	300	10/90

A physical mixture of dipyrindamole and mannitol was prepared using a spatula and mortar.

X-Ray Powder Diffraction

X-ray powder diffraction (XRPD) was performed using CuK α radiation with a wavelength of 1.5405 Å at 40 kV and 40 mA from an X'Pert PRO MPD diffractometer (PANalytical, Almelo, The Netherlands). The samples were scanned from 4 to 60° 2 θ with a step size of 0.008° and a time per step of 35 s.

Scanning Electron Microscopy

SEM pictures were taken using a JEOL JSM 6301-F microscope (JEOL, Japan). The samples were dispersed on top of double-sided sticky carbon tape (Agar scientific, Essex, United Kingdom) on metal disks and coated with a thin layer of gold/palladium (Leica) in a Leica EM SCD 050 sputtering device. The acceleration voltage used was 4.0 kV.

Surface Brunauer, Emmet, and Teller-Isotherm Determination

Before analysis, the powder samples were filled into .25-inch sample tubes and dried with nitrogen gas using a VacPrep 061 (Micromeritics, Norcross, U.S.A.). Thereafter, the average surface area was determined using a Tristar 3000, Micromeritics (Norcross, U.S.A.) BET.

Laser Diffraction

The particle size of the pure dipyrindamole was determined by laser diffraction. Small quantities dipyrindamole were dispersed by using a RODOS dispersing system (Sympatec GmbH, Clausthal-Zellerfeld, Germany) at 1.0 bar. Then the geometric particle size distribution was determined with a Sympatic HELOS compact model KA laser diffraction apparatus (Sympatec GmbH, Clausthal-Zellerfeld, Germany). A 100-mm lens was used, and calculations were based on the Fraunhofer theory (23).

Confocal Laser Scanning Microscopy

CLSM images were obtained using a Leica TCS SP2 microscope (Leica, Mannheim, Germany) with an Argon laser (excitation wavelength 458 nm). HCX PL APO CS 63x NA 1.4 (for the freeze-dried samples) and 40x NA 1.25 (for the physical mixture) oil objectives were used. Both dipyrindamole and mannitol were excited at 458 nm. To obtain the fluorescent image of the dipyrindamole crystals, emission was measured at a wavelength of 482–551 nm. To

obtain a brightfield reflection image of complete powder, scattered light was detected at a wavelength of 449–471 nm. To increase the signal-to-noise ratio, the frame average of six scans was used to produce one image. Since the particle size of certified fluorescent beads was similar in 3-D and 2-D images (data not shown), 2-D images were used to determine the particle size of drug in the samples. Furthermore, since the optical slice thickness (axial resolution) (calculated by Eq. 1, in which d is the optical slice thickness and an airyunit (p) of 1, a refractive index (n) of 1.479 (oil), an excitation wavelength (λ) of 458 nm, and a NA of 1.4 (63x lens) are used) is at least 400 nm and therefore larger than the expected radius of the nanoparticles, the place where the imaging plane intersects the particles does not influence the measured particle size.

$$d = \frac{p \cdot n \cdot \lambda_{exc}}{NA^2} \quad (1)$$

According to the Nyquist criterion (24) and the Huygens (Huygens, SVI) specifications, the sampling density should be a quarter of the resolution of the lens. Since the numerical aperture of the 63x lens is 1.4, the theoretical resolution of this lens is 196 nm. Similarly, the numerical aperture of the 40x lens is 1.25, and the theoretical resolution of this lens is 219 nm. Consequently the ideal pixel size is 49 and 55 nm, respectively. However, since most of the particles in the physical mixture are large, a pixel size of approximately 183 × 183 nm was more suitable and therefore used for images recorded with the 40x lens. The pixel size of the images taken with the 63x lens was, according to the Nyquist criterion, 50 × 50 nm. The digital images were recorded in a 2,048 × 2,048 resolution.

Samples were prepared by using a spatula to spread the powders onto a cover glass (glass thickness of 0.13–0.17 mm, complying with the optical requirements of the objectives). Only the cover glass was used during the CLSM measurement.

Image Analysis

To increase the signal-to-noise ratio, the obtained fluorescent CLSM pictures were first deconvoluted using Classical Maximum Likelihood Estimation algorithm and a measured point spread function (PSF) in the Huygens Professional 3.6 software from Scientific Volume Imaging. ImageJ 1.41n (National Institutes of Health, USA) was used to change the deconvoluted images into binary images and to measure the surface area of the particles. The threshold for the grayscale to binary conversion was calculated by the automatic thresholding function in ImageJ. To exclude the counting of single pixels, originating from noise, only

Table II Particle Size of Certified Fluorescent Beads Measured and Analyzed According to the Protocol. The Given Measured Bead Size is the Mean \pm Standard Deviation of Five Samples

Specified beads size (μm)	Measured bead size (μm)
0.49	0.45 ± 0.12
1.1	1.2 ± 0.1
4.0	4.2 ± 0.4

particles with a surface area larger than an area of 4 pixels were measured. Since the total surface area of particles at the edge can not be determined, these particles were excluded from analysis. The average surface area of each individual particle was measured. Finally, the volume median diameters were calculated by assuming that the particles were spherical.

Validation

To validate whether this protocol can be used to measure the particle size reliably, suspensions of certified fluorescent beads of $0.18 \mu\text{m}$ (subresolution) $0.49 \mu\text{m}$, $1.1 \mu\text{m}$, and $4.0 \mu\text{m}$ were mounted on a cover glass. After the solvent was removed by evaporation under atmospheric conditions, the size of the beads was determined and analyzed according to the protocol as described in the “Confocal Laser Scanning Microscopy” and “Image Analysis” sections.

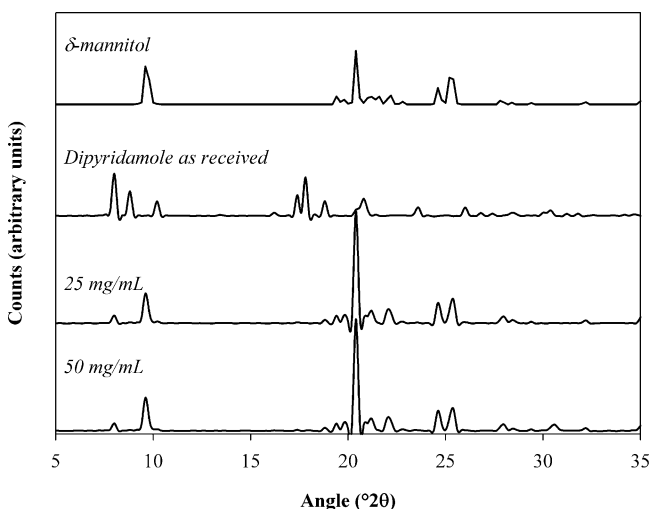


Fig. 1 X-ray diffraction patterns of δ -mannitol, dipyridamole as received, and the dispersions that were prepared freeze-drying from solutions containing 25.0 and 50.0 mg/mL dipyridamole in TBA. In the patterns of the solid dispersions, the major dipyridamole peak at $8.1^\circ 2\theta$ is clearly visible, but also minor dipyridamole peaks at 8.9 , 10.3 , 18.8 , 20.9 , 23.5 , and $26.1^\circ 2\theta$ were found. Both dispersions contained 10% w/w dipyridamole in mannitol.

Tabletting

The obtained powders were compressed into 9-mm round and flat tablets having a weight of 100 mg on a ESH compaction apparatus (Hydro Mooi, Appingedam, The Netherlands). The used compaction rate was 5 kN/s, and the maximum compaction load was 5 kN. The tablets were stored in a vacuum desiccator over silica gel at room temperature for at least one day before further processing.

Dissolution

The dissolution behavior of dipyridamole from the tablets was determined by using a USP dissolution apparatus II (Sotax AT 7, Basel, Switzerland). As dissolution medium 1 L of a pH 6.8 phosphate buffer with 0.05% w/v sodium

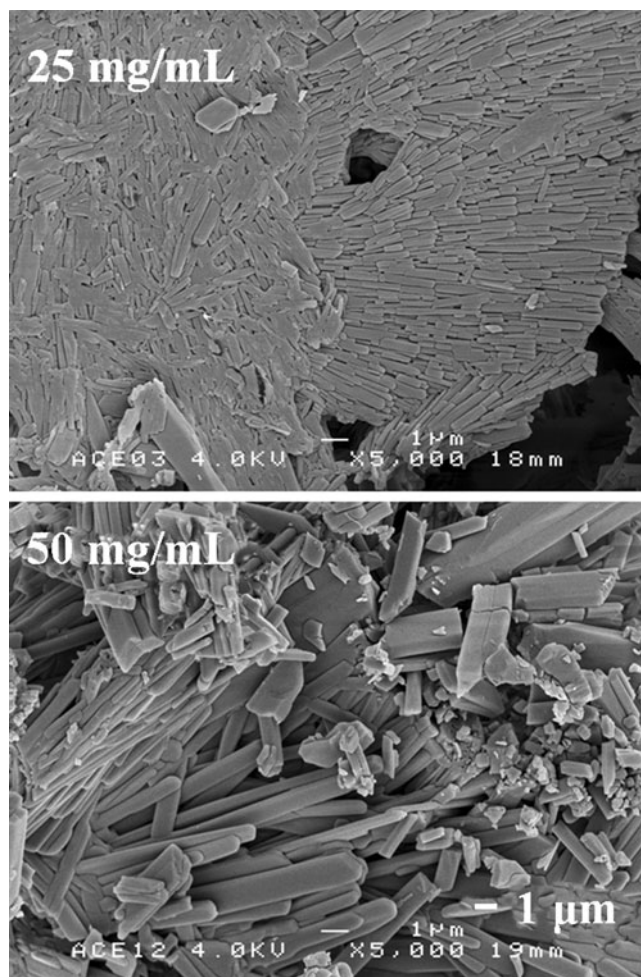


Fig. 2 SEM pictures of two controlled crystallized dispersions. Both contain 10% w/w dipyridamole in mannitol, but one was prepared from a solution containing 25.0 mg/mL dipyridamole in TBA (top), while the other was prepared from a solution containing 50.0 mg/mL dipyridamole in TBA (bottom). Both pictures have a magnification of 5000x.

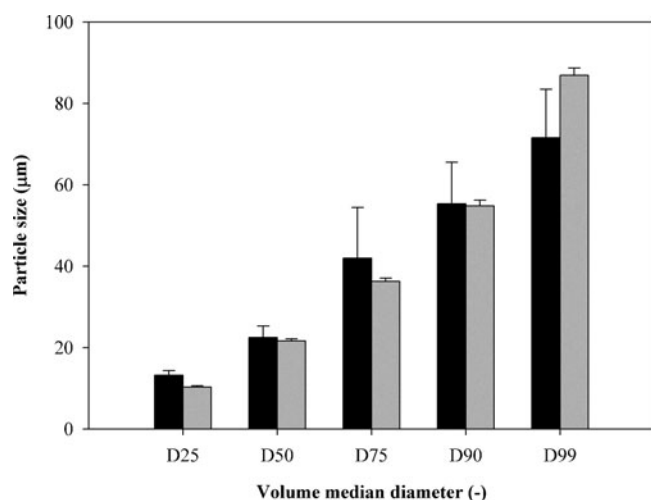


Fig. 3 A comparison between the particle size obtained by CLSM (black bars) and by laser diffraction (grey bars). The particle size obtained by CLSM is the mean \pm standard deviation of three samples. From each sample, 50 images were acquired; per sample, more than 2,000 particles were measured. The particle size obtained by laser diffraction is the mean \pm standard deviation of three measurements.

dodecyl sulphate at a temperature of 37°C was used. The paddle speed was set at 100 rpm. The concentration of dipyrindamole was measured spectrophotometrically (Evolution

300 UV-VIS spectrophotometer, Thermo Fisher Scientific, Madison, U.S.A.) at a wavelength of 285 nm.

RESULTS

Validation

To validate the image acquisition and analysis protocols, the size of certified fluorescent beads was determined. First, subresolution beads (175 nm) were measured. The detected resolution was close to the theoretical resolution of the microscope. Second, beads of 0.5, 1.0, and 4.0 μm were measured. The results found for the certified beads were close to the specified size of these beads (Table II), thus indicating that the described protocol can be used to measure the particle size reliably.

Physicochemical Characterization of the Dispersions

To determine the crystallinity of the obtained dispersions, XRPD was used. Differential scanning calorimetry, which is a common technique to quantify crystallinity, could not be used because the melting point of dipyrindamole and mannitol are almost equal to each other (163°C and 166°C

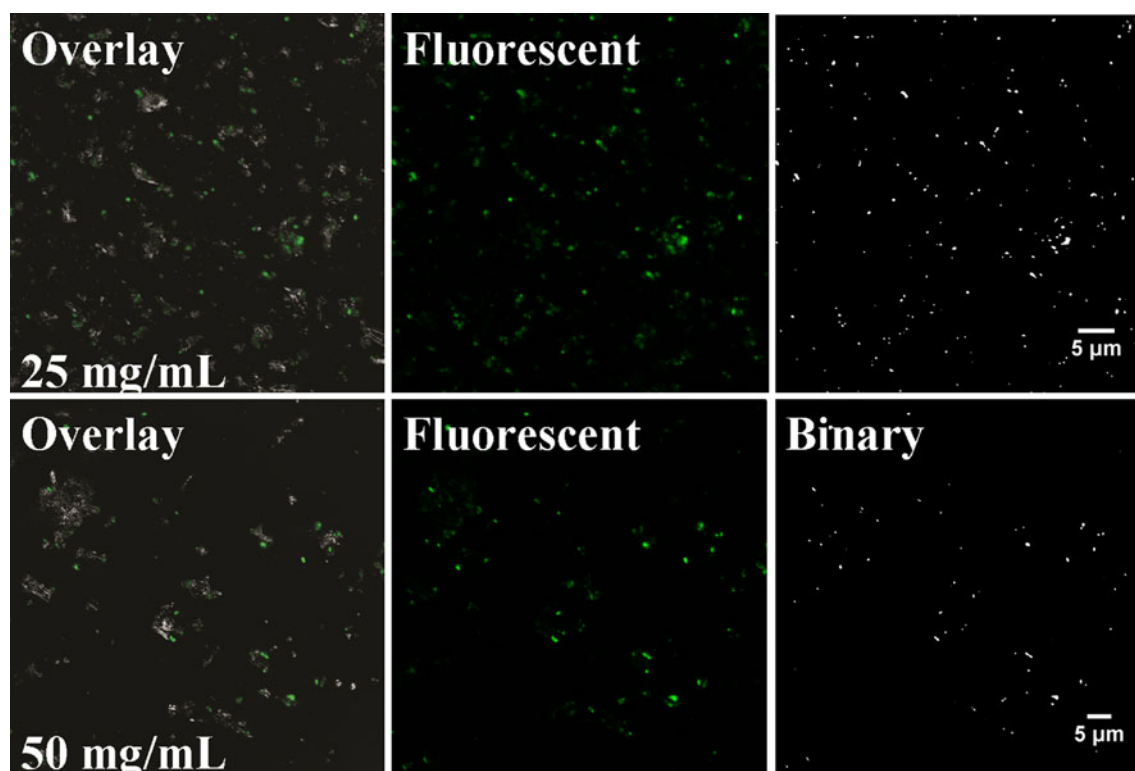


Fig. 4 Examples of a merged image of the brightfield reflection image and fluorescent dipyrindamole images (left), fluorescent images (middle), and binary images (right) of the controlled crystallized dispersions obtained from the solution containing 25 mg/mL (top) and 50 mg/mL (bottom) dipyrindamole in TBA. Both controlled crystallized dispersions contain 10% w/w dipyrindamole in mannitol.

respectively (21,25)). Consequently, the peaks in the thermogram overlap; therefore, the degree of crystallinity could not be determined. However, the XRPD patterns clearly revealed the major dipyrindamole peak at $8.1^\circ 2\theta$, other smaller dipyrindamole peaks, and peaks corresponding to δ -mannitol. This indicates that the obtained dispersions consisted of crystalline dipyrindamole and δ -mannitol (Fig. 1).

SEM analysis of CCDF-generated nanoparticles revealed increased particle sizes with increasing concentrations of dipyrindamole in TBA and mannitol in water (Fig. 2). The BET results showed that the particles obtained from the less concentrated solutions had a larger surface area ($4.6 \text{ m}^2/\text{g}$) than the particles obtained from the more concentrated solutions ($3.7 \text{ m}^2/\text{g}$). These results agree with the SEM findings and are an indication that the particle size is smaller when the samples are freeze-dried from less concentrated solutions.

Comparison Between Laser Diffraction and CLSM

First, it was validated whether CLSM can be used to determine the particle size of the autofluorescent drug while the drug is mixed with a second component. Thereto the pure drug crystal size as determined by laser diffraction was compared with the dipyrindamole crystal size in a physical mixture as determined by CLSM. The fluorescent dipyrindamole signal and the reflected light could easily be separated from each other by CLSM (data not shown). By CLSM analysis, the particle size of the pure drug was found to be similar to the size of the unprocessed drug in the physical mixture (Fig. 3). The most frequently used value to indicate the particle size, the D_{50} value, was found to be $21.7 \pm 0.5 \mu\text{m}$ (mean \pm standard deviation of 3 samples) and $23.9 \pm 2.8 \mu\text{m}$ (mean \pm standard deviation of 3 sets of 50 images; each set consisted of 3,251–4,826 particles) by laser diffraction and CLSM, respectively, for the unprocessed drug. These results indicate that CLSM in combination with the image analysis can be used to determine the particle size of an autofluorescent drug, even though it is mixed with a second component.

Particle Size Analysis and Dissolution

The two previously described dispersions were used to test whether CLSM can also be used as an analytical tool to determine the size of fluorescent drug crystals in solid dispersions. Also in these samples, the dipyrindamole and mannitol could be clearly distinguished from each other by CLSM, and the fluorescent dipyrindamole signal could be separated from the mannitol signal (Fig. 4). After deconvolution, the grey-scale images were converted into binary images. The volume-based particle size distribution was calculated from the binary images.

The calculated particle size distributions do not only show a clear difference in particle size between the physical mixture and the crystallized dispersions, but also between the two crystallized dispersions (Fig. 5a). The D_{50} of dipyrindamole in the physical mixture was found to be $22 \mu\text{m}$, while the size was 0.7 and $1.3 \mu\text{m}$ for the crystals in the dispersions prepared from the less concentrated and more concentrated solutions, respectively.

Although dissolution experiments can not be used to quantify the drug crystal size, differences between drug crystal sizes are reflected in differences in dissolution rate. The dissolution experiments showed that the dissolution rate of dipyrindamole was higher from the controlled crystallized dispersions than from the physical mixture (Fig. 5b). Furthermore, it can be seen that the dissolution

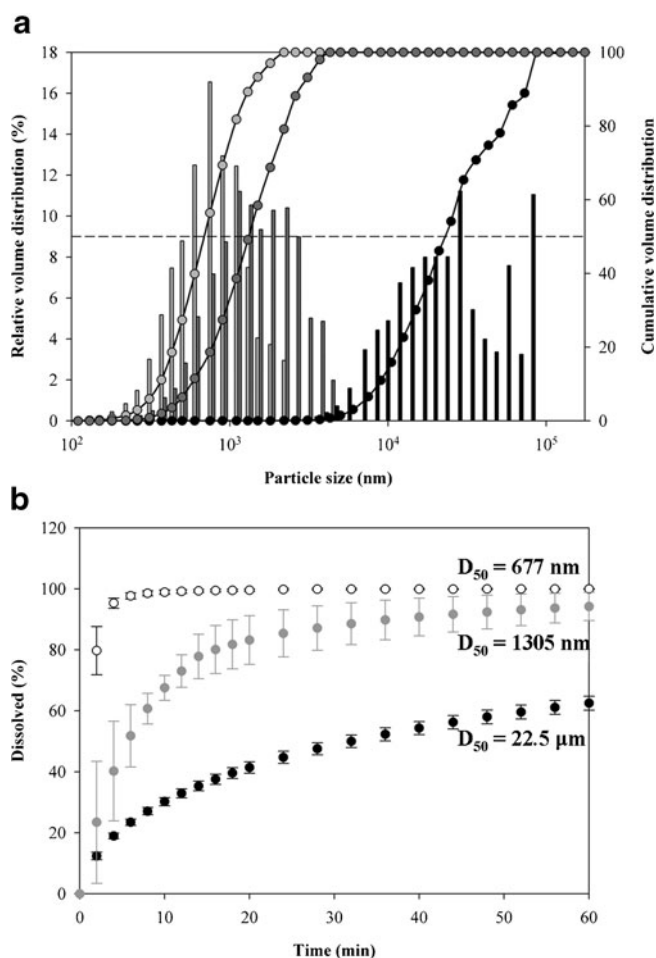


Fig. 5 (a) Particle size distribution of the crystalline dispersions obtained from the 25 mg/mL (light grey) and 50 mg/mL (dark grey) dipyrindamole in TBA solution and the physical mixture (black). (b) Dissolution profiles of dipyrindamole from tablets composed of the physical mixture (filled circle) and controlled crystallized dispersions. The dispersions were prepared from a solution containing 25 mg/mL (white circle) and 50 mg/mL (filled circle) dipyrindamole in TBA. The D_{50} -values in the figure are the values as determined in (a). All tablets contained 10% w/w dipyrindamole ($n = 3-6$; mean \pm standard deviation).

rate was faster when the crystalline dispersion was prepared from the less concentrated solutions. Since all samples were crystalline, a higher dissolution rate indicates smaller crystals. Therefore, it can be concluded that the CLSM findings, which show that the dipyrindamole crystals from the less concentrated solutions are the smallest, are in agreement with the results of the dissolution experiments.

DISCUSSION

In this study, we showed that CLSM, in combination with a two-step image analysis process, can be used as a tool to determine the particle size of autofluorescent drug crystals in the solid state. To validate this, first the pure dipyrindamole crystal size was determined by laser diffraction analysis. The found crystal size was compared to the size of the same drug crystals physically mixed with mannitol as determined by CLSM. Both methods showed a similar particle size distribution, indicating that the combination of CLSM and image analysis can be used to determine the crystal size of dipyrindamole that is mixed with a second component.

In a previous study (11), we developed CCDF as a novel process to prepare drug nanocrystals. In another study (12), we showed that the size of the drug crystals was limited to the size of the interstitial spaces between the frozen solvent crystals. We hypothesized in this study that when less concentrated solutions are freeze-dried, more solvent crystals and therefore smaller interstitial spaces are formed, and consequently smaller drug crystals will be formed.

The results of the BET measurements suggested that the particles obtained from the less concentrated solutions were indeed smaller than the particles obtained from the more concentrated solutions. Furthermore, the SEM pictures suggested that the particles obtained from the less concentrated solutions were of sub-micron size, while the particles from the more concentrated solutions were larger than a micrometer. However, both methods can not distinguish the drug from the matrix.

The CLSM analysis, on the other hand, can distinguish between drug and matrix, and it can be used to quantify the drug crystal size in the crystalline dispersion. It showed that the crystals in the dispersion prepared from the less concentrated solution were of sub-micron size, whereas the crystals in the dispersion prepared from the more concentrated solution were approximately 1.3 μm .

This trend in drug crystal size was in agreement with the dissolution behavior of the tablets prepared from the physical mixture and the freeze-dried products. Since the pure drug, but also both freeze-dried dispersions, are all crystalline, differences in dissolution rate can be ascribed to differences in drug crystal size. Therefore, the dissolution tests showed that the dipyrindamole crystals obtained from the less

concentrated solutions were indeed smaller than the dipyrindamole crystals from the more concentrated solutions.

These results indicate that CLSM is a useful technique to determine the drug crystal size in a powder mixture. The fact that in the crystallized dispersions sub-micron-sized particles were analyzed and in the physical mixture particles of several tens of micrometers indicates that the CLSM method can be used to measure the particle size over a size range covering several orders of magnitude. Furthermore, the particle size of only one of the components in a mixture or dispersion, instead of that of the combination, can be determined. A limitation of the method is that it is limited to autofluorescent drugs. However, when the drug of interest is autofluorescent, CLSM could be a valuable tool.

CONCLUSION

In conclusion, CLSM can be used to determine the drug crystal size of an autofluorescent drug in a powder mixture independent from the mode of incorporation. Advantages are that it can be used to determine the drug crystal size in solid state and that the size of one component in a mixture or dispersion can be determined. Furthermore, CLSM can be used to determine the size of crystals of several hundreds of nanometers to tens of micrometers. A limitation is that this method can only be applied to autofluorescent compounds. In addition to this, we showed that the drug crystal size in the crystalline dispersion, prepared by CCDF, could be controlled by the concentration of drug and matrix in the initial solution.

ACKNOWLEDGMENTS

This research was performed within the framework of project T5-105 of the Dutch Top Institute Pharma. The authors would like to thank P. Pfaffenbach (Solvay Infra Bad Hönningen GmbH, Hannover, Germany) for his assistance on XRPD analysis.

Open Access This article is distributed under the terms of the Creative Commons Attribution Noncommercial License which permits any noncommercial use, distribution, and reproduction in any medium, provided the original author(s) and source are credited.

REFERENCES

1. Lipinski CA *et al.* Experimental and computational approaches to estimate solubility and permeability in drug discovery and development settings. *Adv Drug Deliv Rev.* 2001;46:3–26.

2. Amidon GL *et al.* A theoretical basis for a biopharmaceutical drug classification: the correlation of *in vitro* drug product dissolution and *in vivo* bioavailability. *Pharm Res.* 1995;12:413–20.
3. Lobenberg R, Amidon GL. Modern bioavailability, bioequivalence and biopharmaceuticals classification system. New scientific approaches to international regulatory standards. *Eur J Pharm Biopharm.* 2000;50:3–12.
4. Curatolo W. Physical chemical properties of oral drug candidates in the discovery and exploratory development settings. *Pharm Sci Technol Today.* 1998;1:387–93.
5. Blagden N *et al.* Crystal engineering of active pharmaceutical ingredients to improve solubility and dissolution rates. *Adv Drug Deliv Rev.* 2007;57:617–30.
6. Hu J, Johnston KP, Williams 3rd RO. Nanoparticle engineering processes for enhancing the dissolution rates of poorly water soluble drugs. *Drug Dev Ind Pharm.* 2004;30:233–45.
7. Jinno J *et al.* *In vitro-in vivo* correlation for wet-milled tablet of poorly water-soluble cilostazol. *J Control Release.* 2008;130:29–37.
8. Möschwitzer J *et al.* Development of an intravenously injectable chemically stable aqueous omeprazole formulation using nanosuspension technology. *Eur J Pharm Biopharm.* 2004;58:615–9.
9. Hou D *et al.* The production and characteristics of solid lipid nanoparticles (SLNs). *Biomaterials.* 2003;24:1781–5.
10. Noyes AA, Whitney WR. The rate of solution of solid substances in their own solutions. *J Am Chem Soc.* 1897;19:930–4.
11. de Waard H, Hinrichs WLJ, Frijlink HW. A novel bottom-up process to produce drug nanocrystals: controlled crystallization during freeze drying. *J Control Release.* 2008;128:179–83.
12. de Waard H *et al.* Controlled crystallization of the lipophilic drug fenofibrate during freeze-drying: Elucidation of the mechanism by in-line Raman spectroscopy. *AAPS J.* 2010;12:569–75.
13. Driscoll DF *et al.* Physicochemical assessments of parenteral lipid emulsions: light obscuration *versus* laser diffraction. *Int J Pharm.* 2001;219:21–37.
14. Keck CM, Müller RH. Size analysis of submicron particles by laser diffractometry-90% of the published measurements are false. *Int J Pharm.* 2008;355:150–63.
15. Verma S, Gokhale R, Burgess DJ. A comparative study of top-down and bottom-up approaches for the preparation of micro/nanosuspensions. *Int J Pharm.* 2009;380:216–22.
16. Wu W, Nancollas GH. Determination of interfacial tension from crystallization and dissolution data: a comparison with other methods. *Adv Colloid Interface Sci.* 1999;79:229–79.
17. Bugay DE. Characterization of the solid-state: spectroscopic techniques. *Adv Drug Deliv Rev.* 2001;48:43–65.
18. Doub WH *et al.* Raman chemical imaging for ingredient-specific particle size characterization of aqueous suspension nasal spray formulations: a progress report. *Pharm Res.* 2007;24:934–45.
19. Pygall SR *et al.* Pharmaceutical applications of confocal laser scanning microscopy: The physical characterisation of pharmaceutical systems. *Adv Drug Deliv Rev.* 2007;59:1434–52.
20. Kostewicz ES *et al.* Forecasting the oral absorption behavior of poorly soluble weak bases using solubility and dissolution studies in biorelevant media. *Pharm Res.* 2002;19:345–9.
21. Patterson JE *et al.* The influence of thermal and mechanical preparative techniques on the amorphous state of four poorly soluble compounds. *J Pharm Sci.* 2005;94:1998–2012.
22. Iuliano L *et al.* Fluorescence quenching of dipyrindamole associated to peroxy radical scavenging: a versatile probe to measure the chain breaking antioxidant activity of biomolecules. *Biochem Biophys Acta.* 2000;1474:177–82.
23. Annapragada A, Adjei A. An analysis of the Fraunhofer Diffraction method for particle size distribution analysis and its application to aerosolized sprays. *Int J Pharm.* 1996;127:219–27.
24. Sibarita J-B. Deconvolution microscopy. In: Rietdorf J, editor. *Microscopy techniques.* Berlin Heidelberg: Springer-Verlag; 2005. p. 1288–91.
25. Burger A *et al.* Energy/temperature diagram and compression behavior of the polymorphs of D-mannitol. *J Pharm Sci.* 2000;89:457–68.